Available online at www.sciencedirect.com
SCIENCE DIRECT
Neural Networks 18 (2005) 497–504
Neural Networks
www.elsevier.com/locate/neunet

2005 Special Issue

Metastability, instability, and state transition in neocortex

Walter J. Freeman[a,*], Mark D. Holmes[b]

[a]University of California at Berkeley, Berkeley, CA 94720, USA
[b]University of Washington, Seattle, WA 98104, USA

Abstract

Mesoscopic patterns of neural activity were sought in multichannel EEGs of rabbits that were trained to respond to conditioned stimuli (CSs) in visual, auditory and somatic modalities. Spatiotemporal patterns were sought of oscillations in the beta and gamma ranges. The techniques required for preprocessing EEGs in search of global patterns were diametrically opposed to those needed for localization of modular EEG signals. Frames were found in the form of intermittent spatial patterns of phase and amplitude modulation (AM and PM) of carrier waves in beta and gamma ranges that served to classify EEG frames with respect to CSs. A model based on the intentional action–perception cycle is proposed to complement the information processing model.

Keywords: Action-perception cycle; EEG field dynamics; Metastability; Neocortex; State transition

1. Introduction

Humans observe and grasp complex events and situations by means of expectations that have the form of theories. A theory determines the techniques of observation, which in turn shape what is observed and understood. The classic case in physics is the wave–particle duality, in which the choice of one or two slits determines the outcome of the observation. A similar situation holds for the classic debates among proponents of competing theories about neocortical dynamics: localization vs. mass action. In one view, cortex is a collection of modules like a piano keyboard, each with its structure, signal, and contribution to behavior. In the other view, the neocortex is a continuous sheet of neuropil in each cerebral hemisphere, which embeds specialized architectures that were induced by axon tips arriving from extracortical sources during embryological development. Cooperative domains of varying size emerge within each hemisphere during behavior that includes the specialized.

Observers of both kinds use electroencephalograms (EEGs) and units to test their models. Localizationists (e.g. Calvin, 1996; Houk, 2001; Llinás & Ribary, 1993; Makeig et al., 2002; Singer & Gray, 1995) analogize the neocortex to a cocktail party with standing speakers; each module gives a signal that, when activated like a voice in a room, by volume conduction occupies the whole head and overlaps other signals. On the assumption of stationarity, the signals can be separated by independent components analysis (ICA) of multichannel EEG recordings. Globalists (e.g. Amit, 1989; Basar, 1998; Freeman, 2000) analogize neocortex to a planetary surface, the storms of which are generated by intrinsic dynamics and modified by the structural features of the surface.

These analogies throw into sharp relief the contrasting assumptions and inferences on which the two theories are based. Further, they justify the different methods by which the EEGs are processed, so that after the processing the two forms of the postprocessed EEG data differ dramatically, each legitimately in support of the parent theory. This is why any description of a brain theory should be prefaced by a review of the methods used to get the data that supports the theory.[1]

* Corresponding author.
E-mail addresses: wfreeman@berkeley.edu (W.J. Freeman), drwjfiii@berkeley.edu (W.J. Freeman), mdholmes@u.washington.edu (M.D. Holmes).

0893-6080/$ - see front matter © 2005 Elsevier Ltd. All rights reserved.
doi:10.1016/j.neunet.2005.06.014

[1] An abbreviated version of some portions of this article appeared in reference Freeman and Holmes (2005), as part of the IJCNN conference proceedings, published under the IEEE copyright.

2. Methods

Raw EEG data must be preprocessed prior to measurement. Here six decisions are summarized that have to be made by localizationists and globalists before they acquire EEG data. The choices are diametrically opposed (Freeman, Burke, & Holmes, 2003; Freeman & Holmes, 2005).

(i) According to localizationists, specified behaviors require activation of selected cortical modules that give signals at specific stages of the behaviors and are otherwise silent. The background EEG is incompatible with this expectation, so they adopt the theory established years ago by Bullock (1969) and Elul (1972) that background EEG is dendritic noise, which is so smoothed by volume conduction, particularly at the scalp, that it has no identifiable spatiotemporal structure. They use time ensemble averaging (TEA) to attenuate the noise in proportion to the square root of the number of repeated stimuli that activate the modules, and to extract the expected signals as event-related potentials (ERPs). Globalists view the background activity as the necessary pre-condition for execution of the specified behavior. That activity is modified by conditioned stimuli in differing ways in various areas of neocortex. The induced modifications are not time-locked to triggering stimuli, so that TEA cannot be used. Instead, spatial ensemble averaging (SEA) is used to extract reference values for sets of phase and amplitude values from multiple EEGs.

(ii) The sensor of choice for localization is the depth microelectrode, because the size of the tip determines the acuity of spatial resolution. For globalization the spatial resolution is determined by the interelectrode distances, so the electrode face to minimize noise should be as large as possible without touching neighbor electrodes.

(iii) Both observers use as many electrodes as possible. Localizationists space their electrodes as far apart as possible to sample from as many modules as they can. Globalists space them closely to avoid spatial aliasing and undersampling of spatial patterns of cortical activity.

(iv) Localizationists sharpen the spatial focus of the signals by high-pass spatial filters such as the Laplacian to correct the smoothing by volume conduction. Globalists use low-pass spatial filters to attenuate contributions that are unique to individual electrodes and enhance the sampling of synchronized field potential activity.

(v) Narrow band-pass filters are favored by localizationists on the premise that modular signals are likely to be bursts at definite frequencies such as 40 Hz. Globalists prefer broad-band filters in expectation that oscillatory signals in EEGs are aperiodic (chaotic).

(vi) Signal sources are localized to modules by fitting equivalent dipoles to the filtered data in order to solve the inverse problem. Global signals are not confined to specific anatomical sites; they are localized not in the Euclidean space of the forebrain but in multi-dimensional N-space, where N is the number of available electrodes. These diametrically opposed choices in data processing lead to widely divergent EEG data, and the data lead to theories that are skew. The two theoretical positions are more complementary than conflicting.

3. Results

3.1. Spatial pattern analysis of intracranial EEG

We define a cortical domain of spatially coherent oscillation in neural activity as a wave packet (Freeman, 1975; Freeman 2003a,b). This mesoscopic neural event has a carrier wave at a characteristic frequency, f_i, that is modulated in the beta or gamma range. In any one-wave packet, the variation in frequency seldom exceeds 5% of mean frequency at peak power, so the spectrum of a wave packet usually has a significant peak, but the peak frequency varies unpredictably in sequential wave packets. The wave packets form and end by state transitions that define their durations, D_T. Each carrier wave is modulated in space and time by a spatial pattern of amplitude, $\mathbf{A}(t)$, that is expressed by a $N\times1$ column vector, and a spatial pattern of phase modulation, $\Phi(t)$, in radians. The form that is taken by $\Phi(t)$ is a right cone in the surface dimensions of cortex (Freeman, 2004a,b) giving half-power diameter, D_X, of the wave packet as the distance to cosine of $\phi_j(t)=0.7$.

The mean phase parameters of wave packets were the peak frequency, f_i, in the beta or gamma range (the temporal phase gradient in rad/s) and the spatial phase gradient, g_k, in rad/mm of the phase, $\phi_{i,j}(t)$ (Table 1 in Freeman, 2005c). The basic parameters calculated from the two measures were the temporal wavelength, W_T in ms/rad and spatial wavelength, W_X in mm/rad. These basic parameters served to estimate three novel parameters: phase velocity, b in m/s$=W_X/W_T$, duration, D_T, and diameter, D_X, of wave packets (Table 2 in Freeman, 2005).

The mean amplitude parameters of wave packets were taken from the spatial patterns of amplitude, $\mathbf{A}(t)$ (Fig. 1C in Freeman, 2005), using the EEGs of the olfactory bulb and the visual, auditory and somatic cortices in response to conditioned stimuli with reinforcement (CS+) and without reinforcement (CS−) after discriminative training. The work demonstrated that spatial AM patterns that were expressed in feature vectors, $\mathbf{A}(t)$, could be classified with respect to CSs (Fig. 2A in Freeman, 2005). The accompanying spatial patterns of phase, $\Phi(t)$ (Fig. 2B in

Freeman, 2005), provided evidence that each wave packet formed by a state transition (Freeman, 2004b).

Analysis of the temporal patterns of classification of AM patterns with respect to CSs showed (Fig. 1) that epochs of high likelihood of correct classification occurred intermittently in the time interval between onsets of the CS and conditioned responses (CR). They were detected by application to sets of 40 trials of a moving window 64–128 ms in duration, which was stepped along the sets of 6 s trials at 16 ms intervals. At each step the %correct classification was calculated and plotted in a graph with trial time on the abscissa. The probabilities of those %values occurring by chance were calculated with the binomial distribution (Barrie, Freeman, & Lenhart, 1996). As shown by the example here in Fig. 1, peaks of high classification occurred just after the onsets of CSs and thereafter at varying intervals. The level of %classification declined through the onsets of the CRs, which we inferred were due to variation in the latencies of later classifiable wave packets called 'jitter' (Tallon-Baudry, Bertrand, Peronnet, & Pernier, 1998).

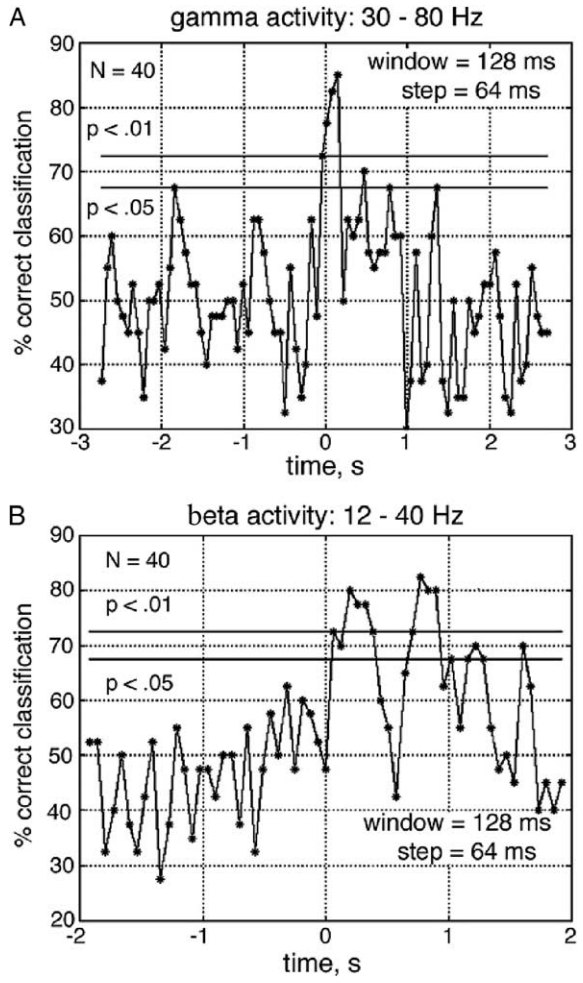

Fig. 1. Probability of %correct classification occurring by chance.

An additional dimension of structure appeared upon analysis of the carrier frequencies in relation to %correct classification. In all cases the multiple EEGs had to be band-pass filtered in order to demonstrate classifiability with respect to CSs. In preliminary studies, the optimal pass band was 20–80 Hz (Barrie et al., 1996). More detailed analysis of the rabbit data showed that correct classification was optimal for wave packets within 140 ms of CS onset when the pass band was in the gamma range (30–80 Hz), whereas wave packets with latencies from CS onsets of 400–600 ms had carrier frequencies in the beta band (12–30 Hz). Wave packets with beta carrier frequencies tended to have longer durations, D_T, larger diameters, D_X, and recurrence rates in the low theta range (3–5 Hz) in contrast to gamma wave packets having recurrence rates in the high theta band (5–7 Hz) (Freeman, 2005).

3.2. Aperiodic phase re-setting of beta-gamma oscillations in state transitions at theta rates

A search was instituted for a marker that could be used to locate wave packets despite the unpredictability of their latencies with respect to the CSs that induced them. To this end the fine temporal structure of the state transitions was explored with the Hilbert Transform (HT), taking advantage of its high temporal resolution of instantaneous frequency and phase (Freeman, 2004a,b). State transitions in broad spatial domains gave rise to the appearance of coordinated discontinuities in phase, which in the time series of the multiple channels are known as 'phase slip' (Pikovsky, Rosenblum, & Kurths, 2001). These jumps were phase re-settings that were followed first by re-synchronization of beta and gamma waves, and then by dramatic increases in analytic amplitude of AM patterns. The optimal measure for classification was found to be given by the mean square of the analytic amplitude, $\underline{A}^2(t)$. (Freeman, 2004b). That increase (Fig. 2A) was preceded by stabilization of the spatial AM pattern. The stability was estimated by calculating the Euclidean distance, $D_E(t)$, between successive points in N-space that represented the feature vectors in 64-space (Freeman, 2004a). High stability was shown by low plateaus in the rate of change of the Euclidean distances between feature vectors.

The most effective tool for locating the spatial AM patterns in the CS–CR time interval was the ratio, $H_E(t) = \underline{A}^2(t)/D_E(t)$, which was named the 'pragmatic information' (Freeman, 2004a). $H_E(t)$ had spikes (Fig. 2B) that gave nearly Gaussian distributions of log H_E (Fig. 3A). Significant segments were demarcated in the EEG by setting a threshold for $H_E(t)$ to locate time epochs of high power and high AM pattern stability. A tuning curve was devised for each subject and data set by systematically varying the $H_E(t)$ threshold and re-calculating %correct values for optimal values (Fig. 3B). Pass bands for filters were also adjusted by classifier-directed optimization.

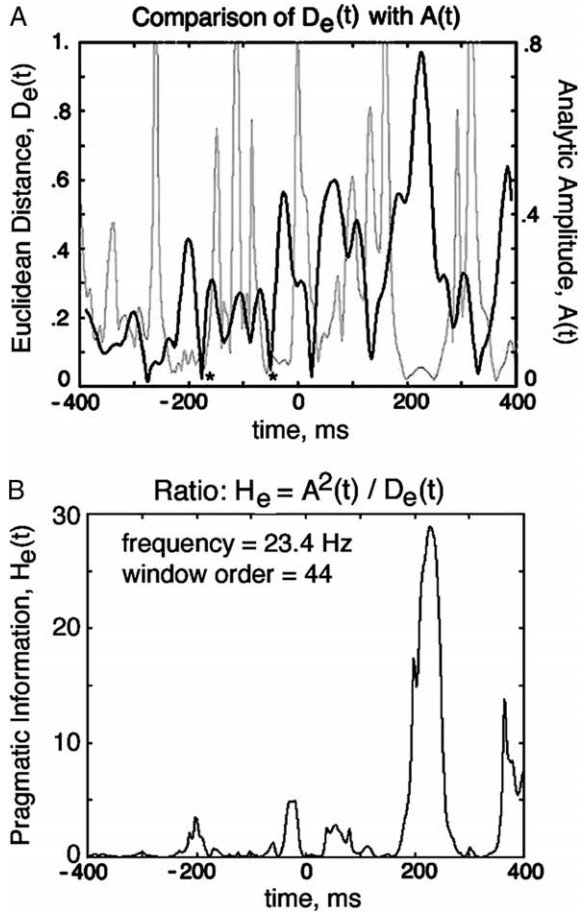

Fig. 2. Parameters derived from applying the Hilbert transform.

Two examples are shown in Fig. 4 of the locations in time of the frames with high $H_E(t)$ in 20 trials of CS+. Similar segments were found in 20 trials of CS−. Frames in the gamma band (A) were most likely to occur immediately after CS onset and were relatively sparse in the pre-stimulus period. The frames in the beta band (B) were distributed in both pre- and post-stimulus epochs but with the greatest likelihood of occurrence later in the CS-CR interval. The times of maximal incidence of frames corresponded to the peaks in %correct classification found by the methods that were illustrated in Fig. 1.

Classification in preceding studies was by the Euclidean distance method applied to 64×1 feature vectors (rms amplitudes of fixed-length segments) in a moving window time-locked across all trials. Each session set was divided into even and odd trials: a training set to calculate two centers of gravity and a test set to calculate the distance in *N*-space of each point to the two centers, then repeating with reversal for cross-validation. Classification was judged to be correct when the distance of a frame on a CS+ trial was shorter to the CS+ center than to the CS− center. This earlier method was limited to two clusters (Fig. 1) and gave no visualization of the distributions of points.

3.3. Classification of wave packets located by $H_E(t)$

An alternative method was to preprocess the feature vectors prior to classification by non-linear mapping (Barrie, Holcman, & Freeman, 1999; Freeman, 2005; Sammon, 1969). The mapping worked unsupervised to project the *M* points in *N*-space representing the whole set of *M* frames into a visualization plane for display, while preserving to a good approximation the distances between the points. An initial plane was defined by the two coordinate axes with largest variances of the data. The $M(M-1)/2$ Euclidean distances were calculated between the points in *N*-space and between the points projected into the plane. An error function was defined by the normalized differences between the two sets of distances. The error was minimized by a steepest gradient.

After optimization of the display in two-space the first three frames after CS onset (Fig. 4) were labeled in sequential order (1, 2, 3) and by CS type, giving six sets of 20 points representing the feature vectors. These points formed clusters owing to similarity of the spatial AM patterns in classes. The center of gravity was calculated

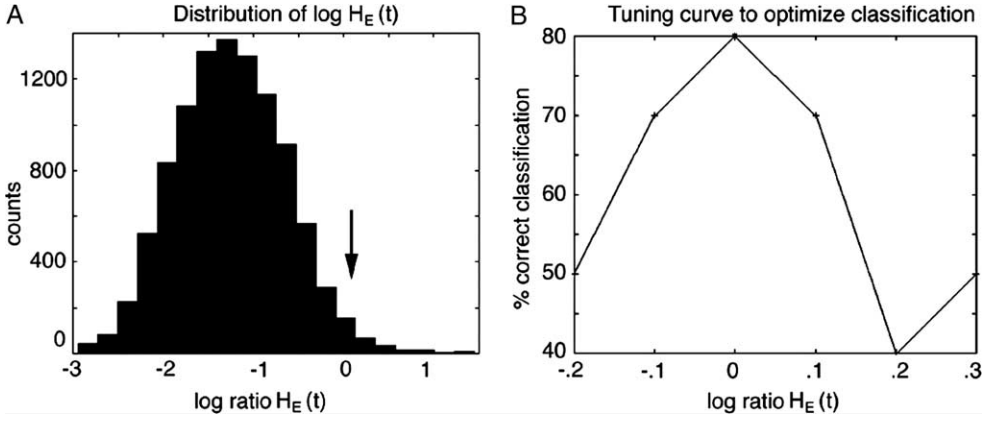

Fig. 3. Use of tuning curves to locate classifiable EEG segments.

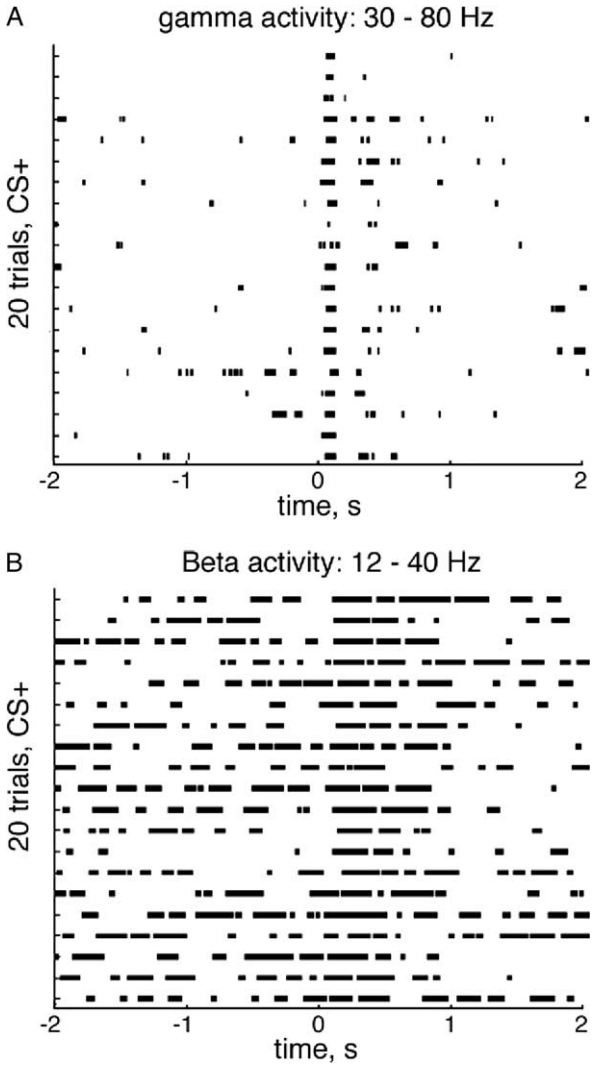

Fig. 4. EEG frames located by $H_E(t)$ with respect to CS onset at 0 s.

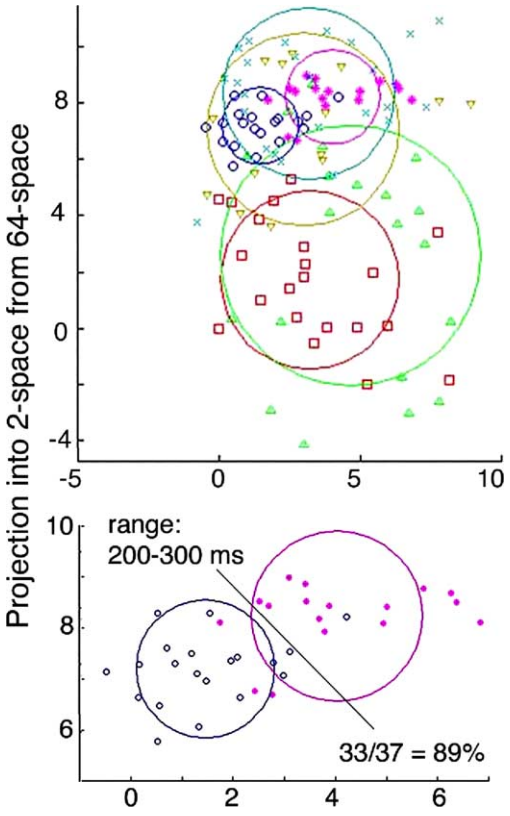

Fig. 5. Feature vectors from 40 trials are represented by points after projection from 64-space into two-space by non-linear mapping.

fo each cluster. Classification of each point was by its Euclidean distance in the 2D projection plane to the nearest projected center of gravity. The classification was correct when the type of the closest center in two-space corresponded to the same type of frame in the six-way classification. For a set of 20 trials of each type, the results were expressed as %correct classification (Barrie et al., 1999; Viana Di Prisco & Freeman, 1985). An example of the output of Sammon's algorithm is shown in Fig. 5A, where the circles indicate the SD of the radial coordinates within a cluster measured with respect to the center in two-space. Pairwise classification was evaluated by assuming linear separability of the clusters. Sammon's method gave flexibility in choosing the number of groups to be classified in terms of the latencies and durations of temporal windows. The level of significance for correct classification was evaluated by applying the same test to the first three feature vectors starting after 1.0 s in the pre-stimulus control period. Classification in the test period was considered to be significant if it exceeded the maximum of level of %correct classification in the control period from all subjects and sessions, which was used as an estimate of $p=0.01$.

The results of classification are summarized as follows. The first of the three gamma frames were significantly classified with respect to CS$\pm$, whereas the first of the three beta frames were not. The second and third of the three gamma frames were not significantly classified, whereas the third beta frames were significantly classified and the second was marginally so ($p<0.05$).

The parameters of the wave packets are summarized in Fig. 6. The mean start latencies of the first test frames (66$\pm$12 ms) were consistent with the known mean start latencies of neocortical-evoked potentials. The latencies of the second (254$\pm$25 ms) and third test frames (448$\pm$41 ms) exceeded those in the control frames in the gamma range on an average by 64 ms; there were no significant differences in the beta range. The recurrence rates from the reciprocals of the mean intervals were in the higher half of the theta range for the gamma band (6.4$\pm$0.3 Hz) and in the lower half for the beta band (4.6$\pm$0.1 Hz).

The durations, D_T, of beta test frames (73$\pm$5 ms) consistently exceeded durations of gamma test frames

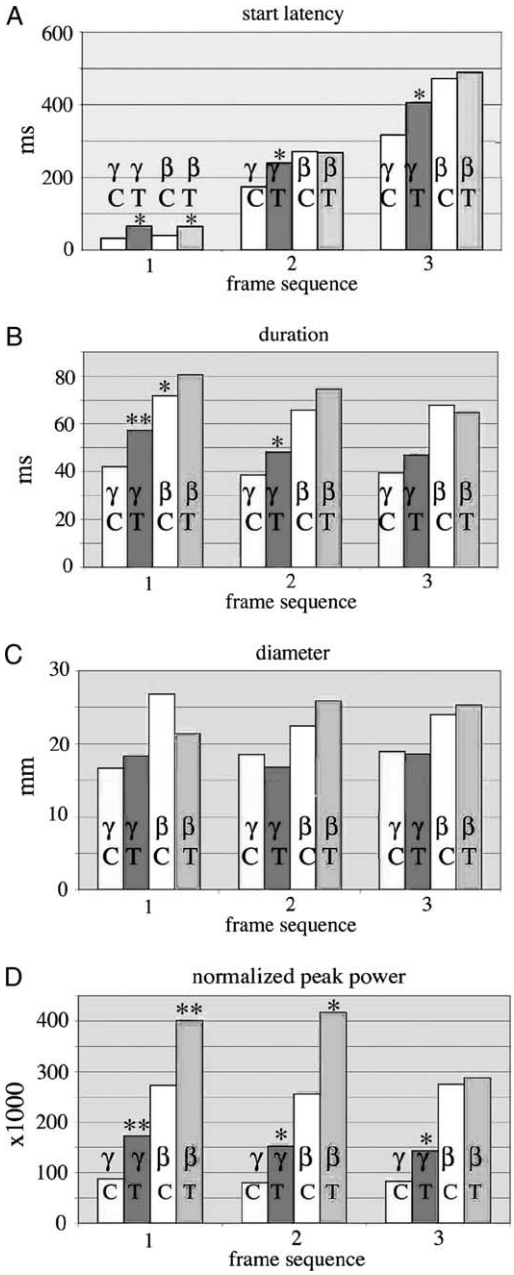

Fig. 6. Summary of wave packet parameters. From Freeman (2005).

(51 ± 7 ms). Diameters, D_X, ranged from 10 to 36 mm, with frames in the beta range consistently exceeding those in the gamma range. There were no significant differences between successive frames or between CS+ and CS−. Peak power normalized with respect to the global mean of EEG from each trial set ranged from 0.07 to 0.60 SD. Normalized peak power in all test frames exceeded two-fold that in all control frames in both pass bands. For test frames but not for control frames in the gamma range peak power decreased from the first to the second frame ($p < 0.05$); a comparable decrease in peak power occurred from the second to the third frame ($p < 0.001$) in the beta range for both CSs, lowering power to the control level.

4. Discussion

Background EEG is notoriously opaque to interpretation and understanding; commonly it is dismissed as noise and is removed by ensemble averaging. Examination of the spatial patterns of phase and amplitude that are carried in multiple EEG signals reveals significant structure in the background EEG that highlights two important properties of neocortex: its instability in respect to multiple sequential state transitions support emergence of frames of patterned activity, and metastability by the recurrence of meaningful patterns.

4.1. Stability, instability, and metastability

The normal neuron is bistable, being either resting or firing. The closer it is brought to its threshold by depolarization the more sensitive it becomes to input. The population homologue is expressed in the asymmetric non-linear gain function (Freeman, 2000) commonly known as the ‘sigmoid curve’. Briefly, absolute stability is guaranteed by an asymptotic approach to threshold on inhibition and limitation by refractory periods on excitation, while instability is guaranteed by the asymmetry of the curve: the maximal gain is displaced to the excitatory side of rest. Excitatory input increases output, and it also increases sensitivity to further input. Sensory stimulation of a cortical population excites some of its neurons and increases their sensitivity. They excite each other so that when a threshold is crossed, the entire population is destabilized. However, when the input ends, the population returns near to its prestimulus state. For local or isolated cortical populations of excitatory and inhibitory neurons, the process can be modeled with a subcritical Hopf bifurcation, so that like the single neuron the cortical population can be regarded as bistable. It appears likely that the large numbers of neural populations interact through the small-world, scale-free synaptic networks of long connections comprising the neuropil of each cerebral hemisphere. Thereby they maintain their background activity at self-organized criticality (Freeman, 2000a,b).

4.2. Interpretation of EEG in terms of action–perception

We interpret our findings in terms of the action–perception cycle of Piaget (1930) and Merleau-Ponty (1945/1962) that expresses intentional behaviour (Freeman, 2001). Our rabbits maintained an intentional stance of expectancy, which required selective attention with fore-knowledge of CSs elicited by the context of the training environment. The expectant state was adaptive and readily updated with new sensory input, which implied that rapid changes in the neural correlates of perception were taking place. We propose that the pre-stimulus beta frames embodied the expectancies in terms of an array of attractor landscapes involving all of the sensory areas and the limbic

system. The impact of CSs destabilized the cortical areas to which they were directed, as manifested in gamma frames, which were more local in space and briefer in time than beta frames. We believe that the time lapse between gamma and beta frames measures the interval that was required for multisensory convergence into the limbic system, passage through the hippocampal formation with integration into the space-time cognitive framework of the rabbits, leading to an up-date of expectancy that was revealed in the later beta frames prior to CR onsets.

In this view the intentional stance is a metastable state within which multiple state transitions occur continuously that make it flexible. Those unstable states and their transitions that are modality-specific are local with smaller size, shorter duration, higher carrier frequencies, and faster frame rates on an average, whereas those unstable cortical states that embody multisensory percepts (Gestalts) have larger size, longer duration, lower carrier frequencies, and lower frame rates. The cortical output to subcortical targets is always local, but the content of the output in the AM patterns is in large part determined by global interactions, so that the neural activity in every sensory area is shaped by contributions from all other areas, as mediated by passage of exchanges through the limbic system by way of its neocortical gateway in the entorhinal cortex.

4.3. Significance of EEG for modeling cognitive processes

The commonly held view of the brain as an information processor is based on the assumption that processing begins with stimulus onset. This is schematized in Fig. 7A.

Each new packet of information, I_{n0}, carried by a stimulus is transduced at receptors into trains of action potentials, which carry it to the appropriate cortex through a series of relays by which it is processed in various ways to I_{n1} and I_{n2}. At the point of injection of the information into the cortex as I_{n3}, it is obscured by background activity. I_{n3} is retrieved by ensemble averaging over repeated trials, thereby verifying that the information has in fact been injected into the cortex albeit in modified form. The difficulty with this view is that cortex appears to lack the neural machinery that would be necessary for temporary storage of multiple sequential trials, summing, and calculation of averages. This set of operations is indicated by the star symbol in Fig. 7. The inadequacy of evidence for this kind of neural processing calls into question the nature and existence of further engineering mechanisms for comparisons of new patterns with those previously stored in memories, I_{nx}, so that an appropriate response might be selected and measured in order to verify that the response contains I_{n3}.

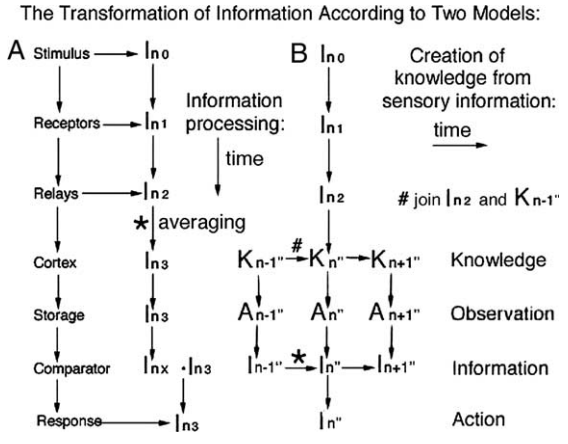

Fig. 7. Transformation of information according to two models. The star represents the operation of averaging. The pound sign represents the operation of the input-induced state transition with accommodation by learning.

An alternative model that is based on the intentional action–perception cycle is schematized in Fig. 7B. The channels for the input of information from the senses to the cortices are the same as for the information processing model. The difference begins at the site of impact of the information onto cortical dynamics as indicated by the pound symbol, #. That symbol represents the state transition by which input destabilizes cortex, selects a basin of attraction in a pre-existing attractor landscape, and modifies the basin and its attractor in a cumulative learning process. The destabilizing input, of course, is the consequence of an intentional act of observation and sampling the environment. The action is the cause of the stimulus, in contrast with the information processing model in which the stimulus is the cause of the response.

The collections of attractor basins in the forebrain are expressions of the memories of the animals and constitute the knowledge base. In an expectant state, the sample that is brought up for testing is denoted $K_{n-1''}$ in Fig. 7B. That state is not directly observable, whereas the emergent spatiotemporal patterns of neural activity are detectable with appropriate sensors for action potentials, EEGs, MEGs, and other images. The observables corresponding to $K_{n-1''}$ are labeled $A_{n-1''}$. The measurements of the observables are accumulated in sets of numbers, which constitute the available information about the observables, $I_{n-1''}$. That numeric information is the basis for the graphs in this and related prior reports, for statistical analyses, and for classification of spatiotemporal patterns with respect to CSs and CRs. However, the information is not in the brains of the animals; it is in the statistical descriptions of the observables and in the models based on the observations.

With the onset of an expected stimulus the receiving cortex is destabilized, an attractor landscape is created, and a selection is made by the CS from the available basins, which is manifested in the AM pattern of a gamma wave packet. The synaptic networks that have been selected for activation in the cortical neuropil are modified by Hebbian and non-Hebbian learning (Freeman, 2000; Kozma & Freeman, 2001), and the selected attractor and its attendant basin are updated, denoted $K_{n''}$ in Fig. 7B. The information

having done its work is then attenuated by the divergent–convergent projections by which cortical output is transmitted (Freeman, 2003a). This inference is based on studies of measurements, $I_{n''}$, of the observables, A_n. The action–perception cycle then repeats giving $K_{n+1''}$, $A_{n+1''}$ and $I_{n+1''}$ based on the action following $K_{n''}$.

In summary, techniques determine the information that is derived by processing raw EEG observations. The high temporal and spatial resolution afforded by the Hilbert transform and high-density electrode arrays have revealed temporal structure in the form of repetitive state transitions and spatial structure in the forms of amplitude and phase modulations of beta and gamma oscillations. The finding that the AM patterns can be classified with respect to CSs well beyond chance levels supports the theory of the action–perception cycle, by which expectancy precedes acts of observation and sensitizes the primary sensory cortices to the several predicted consequences of impending actions. Reception is followed by selection by the sensory input of one of the possible outcomes and updating of the cortical synaptic networks. These ongoing modifications can explain the accommodation of EEG patterns to the environmental conditions.

References

Amit, D. J. (1989). *Modeling brain function: The world of attractor neural networks*. Cambridge, UK: Cambridge University Press.

Barrie, J. M., Freeman, W. J., & Lenhart, M. (1996). Modulation by discriminative training of spatial patterns of gamma EEG amplitude and phase in neocortex of rabbits. *Journal of Neurophysiology*, *76*, 520–539.

Barrie, J. M., Holcman, D., & Freeman, W. J. (1999). Statistical evaluation of clusters derived by nonlinear mapping of EEG spatial patterns. *Journal of Neuroscience Methods*, *90*, 87–95.

Basar, E. (1998). *Brain oscillations 1. Principles and approaches. 2. Integrative brain function, neurophysiology and cognitive operations*. Berlin: Springer.

Bullock, T. H. (1969). The neuron doctrine and electrophysiology. *Science*, *129*, 997–1002.

Calvin, W. H. (1996). *The cerebral code. Thinking a thought in the mosaics of the mind*. Cambridge, MA: MIT Press.

Elul, R. (1972). The genesis of the EEG. *Internal Review of Neurobiology*, *15*, 227–272.

Freeman, W. J. (1975). *Mass action in the nervous system*. New York: Academic Press. Available in electronic form on http://sulcus.berkeley.edu.

Freeman, W. J. (2000). *Neurodynamics. An exploration of mesoscopic brain dynamics*. London: Springer.

Freeman, W. J. (2001). *How brains make up their minds*. New York: Columbia UP.

Freeman, W. J. (2003a). A neurobiological theory of meaning in perception. Part 1. Information and meaning in nonconvergent and nonlocal brain dynamics. *International Journal of Bifurcation Chaos*, *13*, 2493–2511.

Freeman, W. J. (2003b). The wave packet: An action potential for the 21st century. *Journal of Integrative Neuroscience*, *2*, 3–30.

Freeman, W. J. (2004a). Origin, structure, and role of background EEG activity. Part 1. Analytic phase. *Clinical Neurophysiology*, *115*, 2077–2088.

Freeman, W. J. (2004b). Origin, structure, and role of background EEG activity. Part 2. Analytic amplitude. *Clinical Neurophysiology*, *115*, 2089–2107.

Freeman, W. J. (2005). Origin, structure, and role of background EEG activity. Part 3. Neural frame classification. *Clinical Neurophysiology*, *116*, 1118–1129.

Freeman, W. J., Burke, C., & Holmes, M. D. (2003). Aperiodic phase re-setting in scalp EEG of beta-gamma oscillations by state transitions at alpha–theta rates. *Human Brain Mapping*, *19*, 248–272.

Freeman, W. J., & Holmes, M. D. (2005). Temporal discontinuities in neocortical dynamics. *Proceedings of the IJCNN CDROM*.

Houk, J. C. (2001). Neurophysiology of frontal–subcortical loops. In D. G. Lichter, & J. L. Cummings (Eds.), *Frontal–subcortical circuits in psychiatry and neurology* (pp. 92–113). New York: Guilford Publications.

Kozma, R., & Freeman, W. J. (2001). Chaoric resonance: Methods and applications for robust classification of noisy and variable patterns. *International Journal of Bifurcation and Chaos*, 10, 2307–2322.

Llinás, R., & Ribary, U. (1993). Coherent 40 Hz oscillations characterize dream state in humans. *Proceedings of the National Academy of Sciences (USA)*, *90*, 2078–2081.

Makeig, S., Westerield, M., Jung, T.-P., Enghoff, S., Townsend, J., Courchesne, E., et al. (2002). Dynamic brain sources of visual evoked responses. *Science*, *295*, 690–694.

Merleau-Ponty, M. (1945/1962). *Phenomenology of perception (Smith C. trans)*. New York: Humanities Press.

Piaget, J. (1930). *The child's conception of physical causality*. New York: Harcourt, Brace.

Pikovsky, A., Rosenblum, M., & Kurths, J. (2001). *Synchronization—a universal concept in non-linear sciences*. Cambridge, UK: Cambridge University Press.

Sammon, J. W. (1969). A nonlinear mapping for data structure analysis. *IEEE Transactions on Computer C*, *18*, 401–409.

Singer, W., & Gray, C. M. (1995). Visual feature integration and the temporal correlation hypothesis. *Annual Review of Neuroscience*, *18*, 555–586.

Tallon-Baudry, C., Bertrand, O., Peronnet, F., & Pernier, J. (1998). Induced gamma-band activity during the delay of a visual short-term memory task in humans. *Journal of Neuroscience*, *18*, 4244–4254.

Viana Di Prisco, & Freeman, W. J. (1985). Odor-related bulbar EEG spatial pattern analysis during appetitive conditioning in rabbits. *Behavioral Neuroscience*, *99*, 964–978.